Electronic Supplementary Material (ESI) for Journal of Materials Chemistry C.

Supporting Information

Polaron Self-localization in White-light Emitting Hybrid Perovskites

Daniele Cortecchia,[1,2] Jun Yin,[3,4] Annalisa Bruno,[2] Shu-Zee Alencious Lo,[3] Gagik G. Gurzadyan,[3] Subodh Mhaisalkar,[2] Jean-Luc Brédas,[4] Cesare Soci[3,5,*]

[1] *Interdisciplinary Graduate School, Nanyang Technological University, Singapore 639798*

[2] *Energy Research Institute @ NTU (ERI@N), Research Techno Plaza, Nanyang Technological University, 50 Nanyang Drive, Singapore 637553*

[3] *Division of Physics and Applied Physics, School of Physical and Mathematical Sciences, Nanyang Technological University, 21 Nanyang Link, Singapore 637371*

[4] *Laboratory for Computational and Theoretical Chemistry and Advanced Materials, Division of Physical Science and Engineering, King Abdullah University of Science and Technology, Thuwal 23955-6900, Saudi Arabia*

[5] *Centre for Disruptive Photonic Technologies, TPI, Nanyang Technological University, 21 Nanyang Link, Singapore 637371*

[*] Corresponding Author: csoci@ntu.edu.sg

I. Materials Characterization

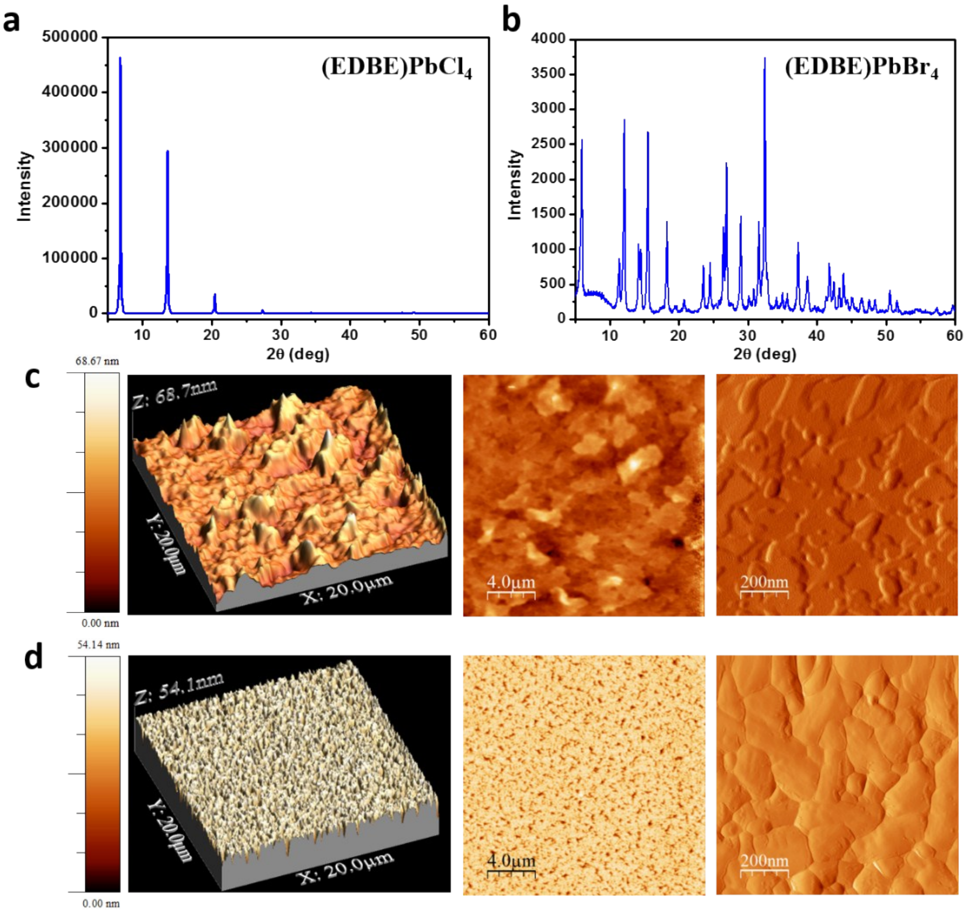

Figure S1| Material characterization. XRD patterns of drop casted films of **a,** (EDBE)PbCl$_4$ and **b,** (EDBE)PbBr$_4$. **c,d**) Atomic force microscopy (AFM) characterization of perovskite thin films. Typical films used for optical characterization deposited from 0.25M DMSO solutions: c) (EDBE)PbCl$_4$, with thickness of 107±11 nm and root mean square roughness $R_{RMS} = 7$ nm; **d**) (EDBE)PbBr$_4$, with thickness 80±10 nm and $R_{RMS} = 6$ nm.

X-ray analysis on drop-casted films confirmed the achievement of the desired phase (EDBE)PbCl$_4$ and (EDBE)PbBr$_4$ in agreement with the previous report on these materials. (EDBE)PbCl$_4$ (**a**), crystallizes as <100>-oriented perovskite with monoclinic crystal system, space group *C*2 and lattice parameters a = 7.748 Å, b = 7.523 Å, c = 13.346 Å, β = 102.68°. The drop casted film shows a strong preferential orientation toward the *00l* direction indicating a perfect alignment of the organic and inorganic sheet parallel to the substrate. (EDBE)PbBr$_4$ crystallizes as <110>-oriented perovskites (**b**) with monoclinic crystal system, space group $P2_1/c$, and lattice parameters a = 6.142 Å, b = 28.906 Å, c = 8.701 Å, β = 91.69° and does not show any strong preferential orientation in the drop-casted film.

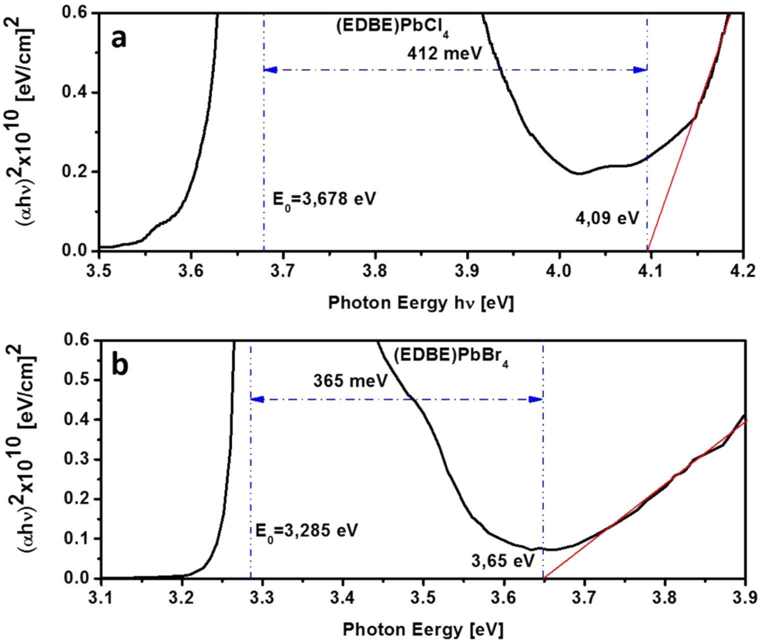

Figure S2| Exciton binding energy determination. Tauc Plots construction and exciton binding energy (EBE) at 78 K for **a,** (EDBE)PbCl$_4$ and **b,** (EDBE)PbBr$_4$. The exciton binding energy was estimated taking the difference between the energy of the 0-0 transition (E_0, see Table S1) and the onset of the high-energy absorption continuum. The extracted EBE is 412 meV and 369 meV for (EDBE)PbCl$_4$ and (EDBE)PbBr$_4$, respectively.

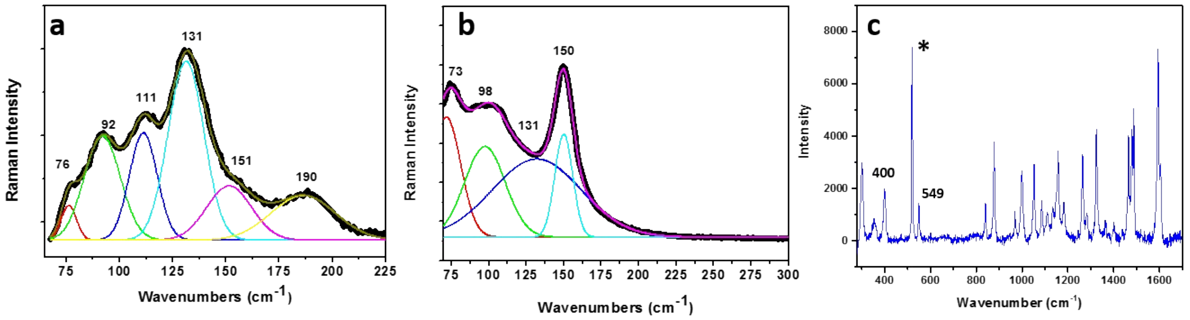

Figure S3| Raman spectra. a) (EDBE)PbCl$_4$ and b) (EDBE)PbBr$_4$: the Raman spectra show the Pb-Cl and Pb-Br stretching indicating the formation of the inorganic framework. (EDBE)PbCl$_4$ spectrum shows peaks at 76, 92, 111, 131 and 190 cm^{-1} while (EDBE)PbBr$_4$ has peaks at 73, 98 and 150 cm^{-1}. c) High energy Raman spectrum of (EDBE)PbCl$_4$, corresponding to the vibrational modes of the organic cations (* indicates the signal from the silicon substrate).

II. Fitting of excitonic absorption with Franck-Condon progression

The fitting of the low temperature (T=78K) excitonic absorption was performed using a Frank-Condon progression.[1,2] The intensities of the vibronic features couple to a phonon according to the equation:

$$I_{0\to n} = I_0 \frac{S^n e^{-S}}{n!} \quad [1]$$

Where I_0 represents the intensity of the transitions, and $I_{0\to n}$ is the transition from the 0 vibronic level of the S_0electronic state to the n^th^ vibronic level in the stateS_1. $I_{0\to n}$ is defined as:

$$I_0 = \sum_{n=0}^{\infty} I_{0\to n} \quad [2]$$

The Huang-Rhys parameter S is defined as:

$$S = \frac{k(\Delta Q)^2}{2\hbar\omega_p} \quad [3]$$

Where k indicates the spring constant, while ΔQ represents the modification in coordination coordinate (upon transition $S_0 \to S_1$). ω_p is the angular frequency of the phonon mode having energy E_p.

The features where modelled with a Voigt profile where WG and WL represent the width of the associated Gaussian and Lorentian, respectively. The fitting was modelled as a series of 2 and 10 Frank-Condon coupled Voigt profiles for $(EDBE)PbCl_4$ and $(EDBE)PbBr_4$, respectively. The other fitting parameters include the E_0 energy corresponding to the 0-0 transition, Huang-Rhys parameter S_n, and the energy of the phonons E_{pn}. We considered a coupling of the electronic transition with 4 phonon modes for $(EDBE)PbCl_4$ and 1 for $(EDBE)PbBr_4$. The fitting was performed by imposing the phonon energies according to the experimental values derived from Raman measurements. For $(EDBE)PbCl_4$ the phonon energies $E_{p1} = 16\ meV$, $E_{p2} = 24\ meV$, $E_{p3} = 49\ meV$, $E_{p4} = 68\ meV$, correspond to the Raman vibrational modes at 131, 190, 400 and 549 cm^{-1}. For $(EDBE)PbBr_4$ the phonon with energy $E_{p1} = 19\ meV$ matches the Raman mode at 150 cm^{-1}.

Table S1| Fitting parameters of the Franck Condon progression. E_0 = energy of the 0-0 transition. S_n=Huang-Rhys factors. WL and WG are the width of the Gaussian and Lorentian associated to the Voigt profile used to model the vibronic features.

	E_0 [eV]	E_{p1} [eV]	E_{p2} [eV]	E_{p3} [eV]	E_{p4} [eV]	S1	S2	S3	S4	WL	WG
(EDBE)PbCl$_4$	3.678	0.016	0.024	0.049	0.068	0.018	0.444	1.098	0.165	0.013	0.027
(EDBE)PbBr$_4$	3.286	-	-	-	-	2.387	-	-	-	0.016	0.024

III. Optical Characterization

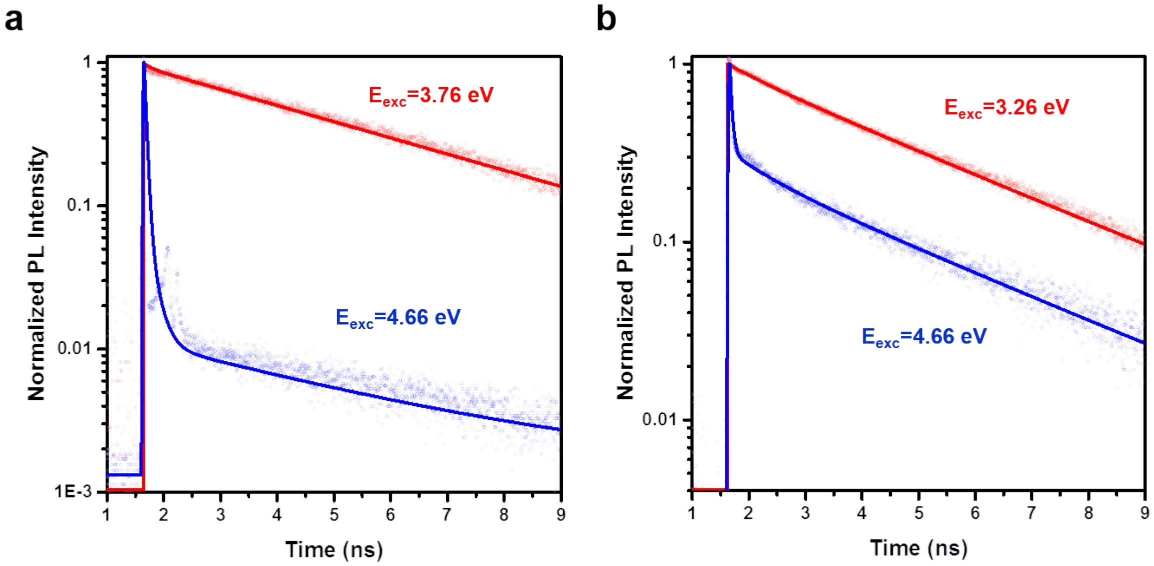

Figure S4| Ultrafast dynamics dependence on excitation energy. a, (EDBE)PbCl$_4$ fluorescence decays after excitation at 4.66 eV (blue) and excitation at 3.76 eV (red) with detection at 2.34 eV. **b,** (EDBE)PbBr$_4$ fluorescence decays upon excitation at 4.66 eV (blue) and 3.26 eV (red) with detection at 2.34 eV.

Table S2| Time resolved photoluminescence (TRPL) parameters for different excitation energy. The characteristic lifetimes (τ) and amplitudes (A) were extracted from the fitting of the dynamics at the probing energy of 2.34 eV.

Material	Excitation Energy (eV)	τ 1 (ns)	A1	τ 2 (ns)	A2	τ 3 (ns)	A3
(EDBE)PbCl$_4$	4.66	0.04	0.93	0.15	0.06	3.8	0.01
	3.76	0.04	0	0.15	0.06	3.8	0.94
(EDBE)PbBr$_4$	4.66	0.04	0.79	0.74	0.04	3.2	0.17
	3.26	0.04	0	0.74	0.09	3.2	0.91

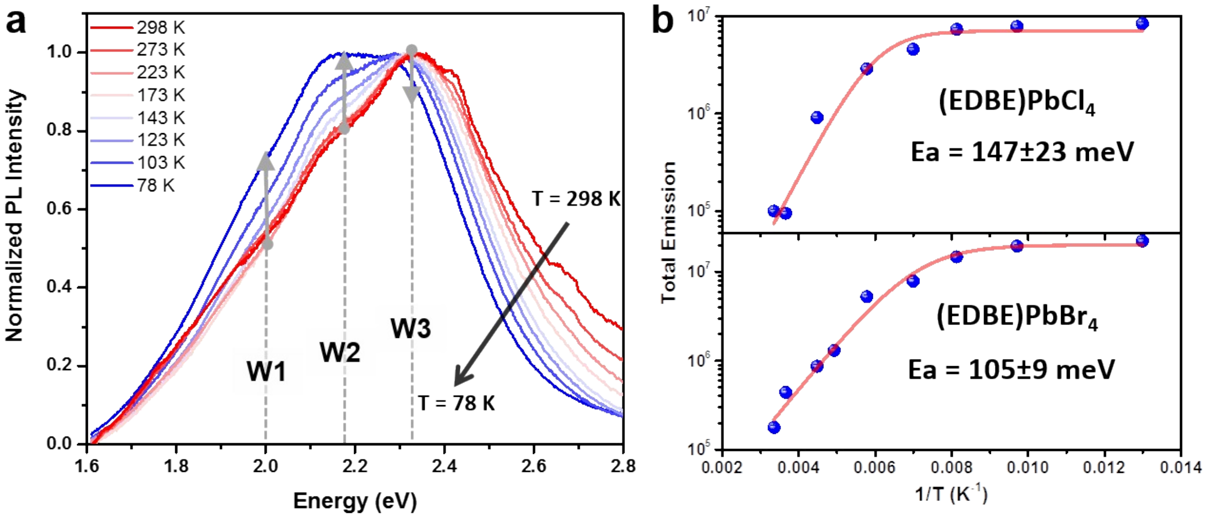

Figure S5| Temperature dependent steady state photoluminescence. a, Evolution of (EDBE)PbCl$_4$ emission profile with temperature (E_{exc} 3.76 eV). The dashed lines indicate the temperature-independent energy of the three principal components (W1=1.96 eV, W2=2.15 eV and W3= 2.34 eV) determined from the principal component fitting of all photoluminescence spectra. **b,** Arrhenius plots of the integrated PL intensity (I) as a function of temperature. The refinement was done using the Arrhenius formula $I = I_0/[1 + a exp(- E_a/kT)]$, where E_a is the activation energy, k is the Boltzmann constant, I_0 is the zero-temperature PL intensity and a represents the strength of the quenching process. The plots are relative to (EDBE)PbCl$_4$ (upper panel) and (EDBE)PbBr$_4$ (lower panel)

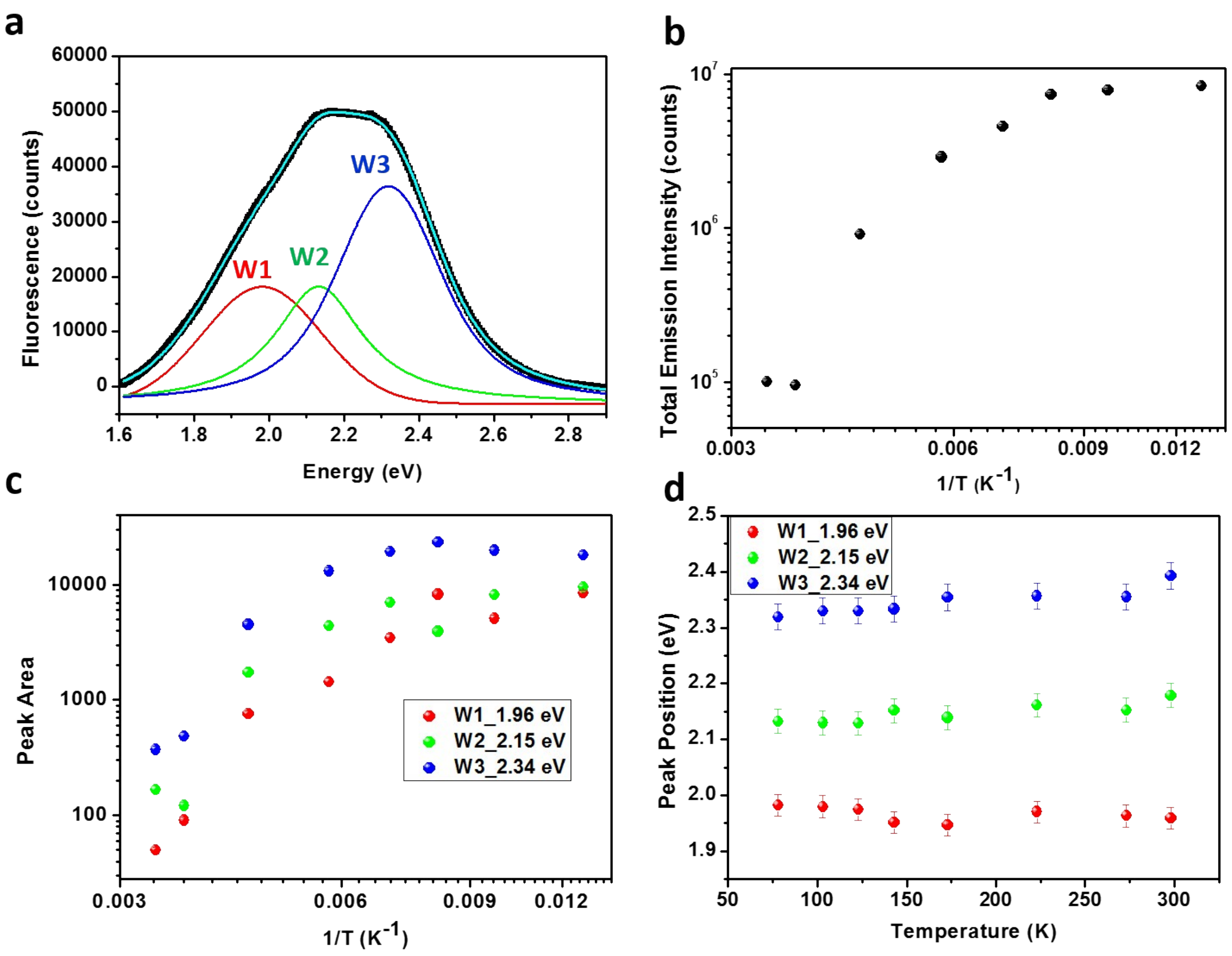

Figure S6| Temperature dependent steady state luminescence of (EDBE)PbCl$_4$. a, Steady state PL at 78 K showing the three components W1, W2, W3 peaked at 1.96 eV, 2.15 eV and 2.34 eV, respectively. **b,** Temperature dependence of total emission intensity, showing increase of almost two orders of magnitude at 78 K. **c,** Area of each PL component respect to temperature, showing the different trend of W1, W2 and W3 during the temperature decrease. **d,** Peak position vs temperature, indicating that W1, W2 and W3 do not shift with temperature, but only their relative intensity is affected.

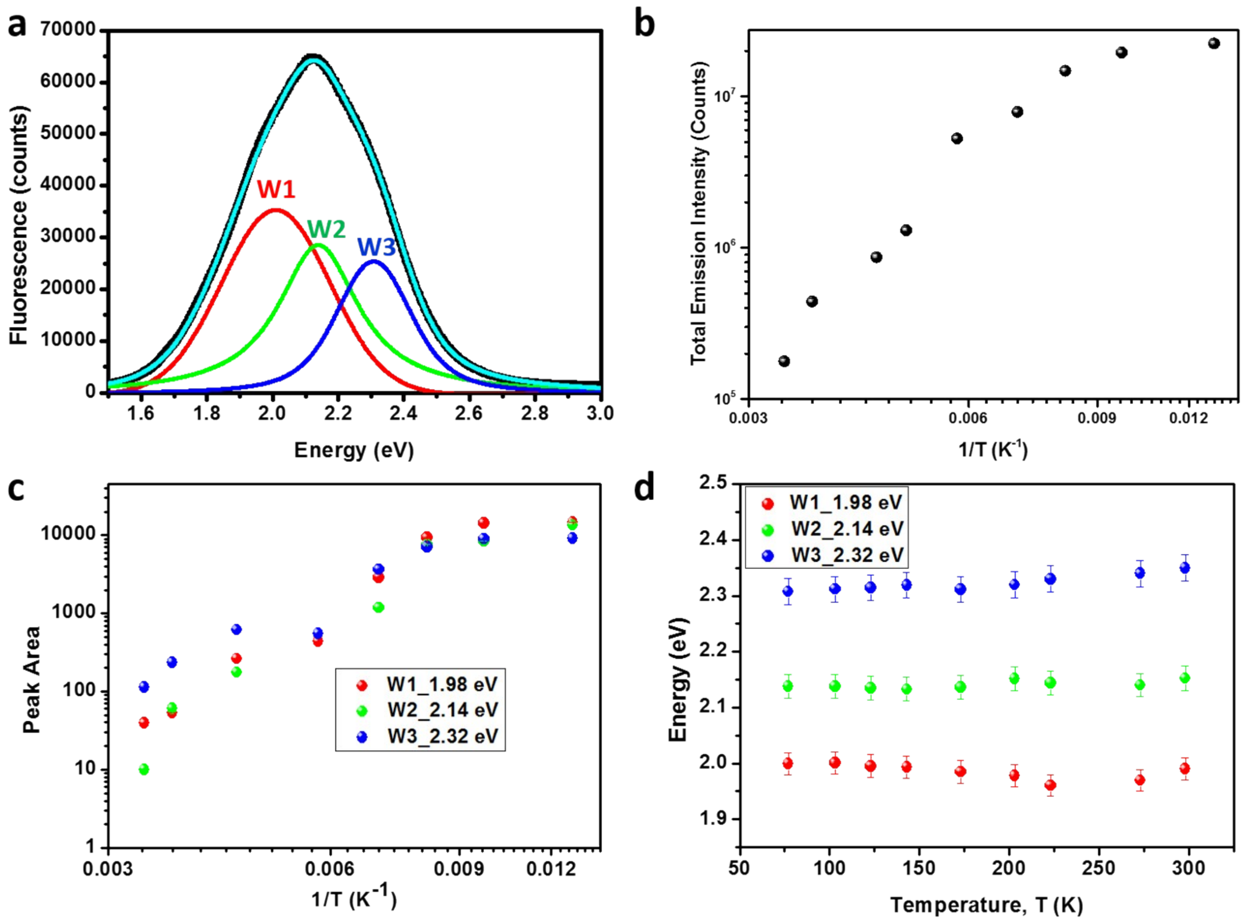

Figure S7| Temperature dependent steady state luminescence of (EDBE)PbBr$_4$. a, Steady state PL at 78 K showing the three components W1, W2, W3 peaked at 1.96 eV, 2.15 eV and 2.34 eV, respectively. **b,** Temperature dependence of total emission intensity, showing increase of almost two orders of magnitude at 78 K. **c,** Area of each PL component respect to temperature, showing the different trend of W1, W2 and W3 during the temperature decrease. **d,** Peak position vs temperature, indicating that W1, W2 and W3 do not shift with temperature, but only their relative intensity is affected.

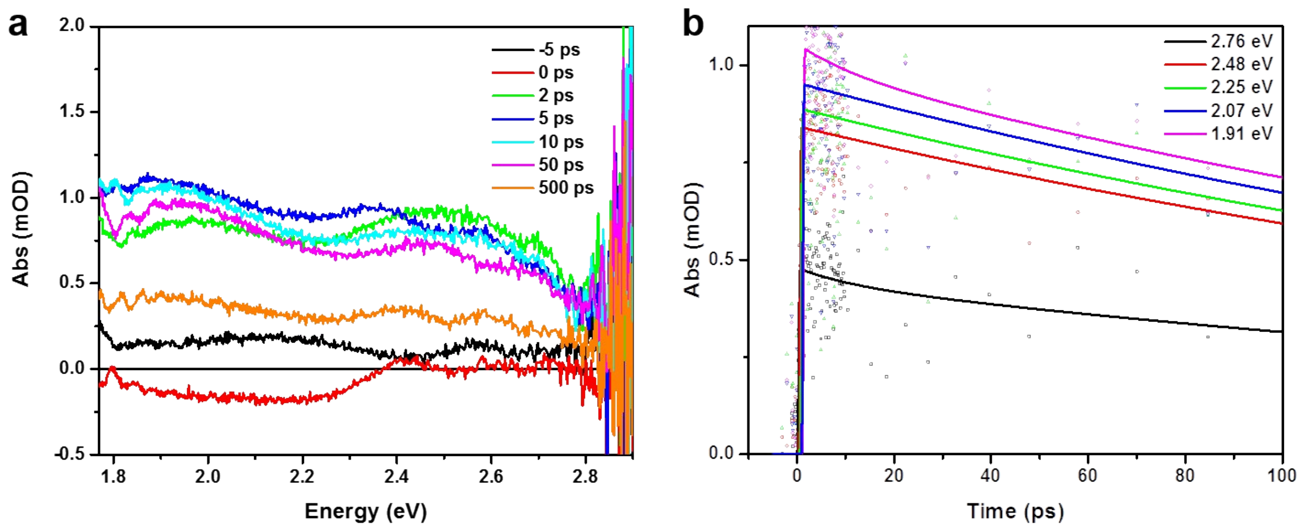

Figure S8| Transient absorption (TA) measurements of (EDBE)PbCl$_4$. a, TA spectra with excitation resonant to the excitonic peak (Eexc = 3.76 eV) and **b,** corresponding decay dynamics at different spectral position. The decays follow a similar dynamic across the whole spectral range.

Table S3| Transient absorption (TA) dynamics fitting parameters for different excitation energy. The characteristic lifetimes (τ) and amplitudes (A) were extracted from the global fitting of 6 decays at different spectral regions using a double exponential decay function. The excitation energy is resonant to the excitonic peak of the perovskite, E_{exc} = 3.76 eV and E_{exc}=3.26 eV for (EDBE)PbCl$_4$ and (EDBE)PbBr$_4$, respectively.

Material	Excitation Energy (eV)	Probe Energy (eV)	τ1 (ps)	A1	τ2 (ps)	A2
(EDBE)PbCl$_4$	3.76	2.76	11.1	0.08	296.4	0.92
		2.48		0.07		0.93
		2.25		0.00		1.00
		2.07		0.04		0.96
		1.91		0.05		0.95
(EDBE)PbBr$_4$	3.26	2.76	9.8	0.46	741	0.54
		2.48		0.51		0.49
		2.25		0.46		0.54
		2.07		0.41		0.59
		1.91		0.19		0.81

IV. Computational Details

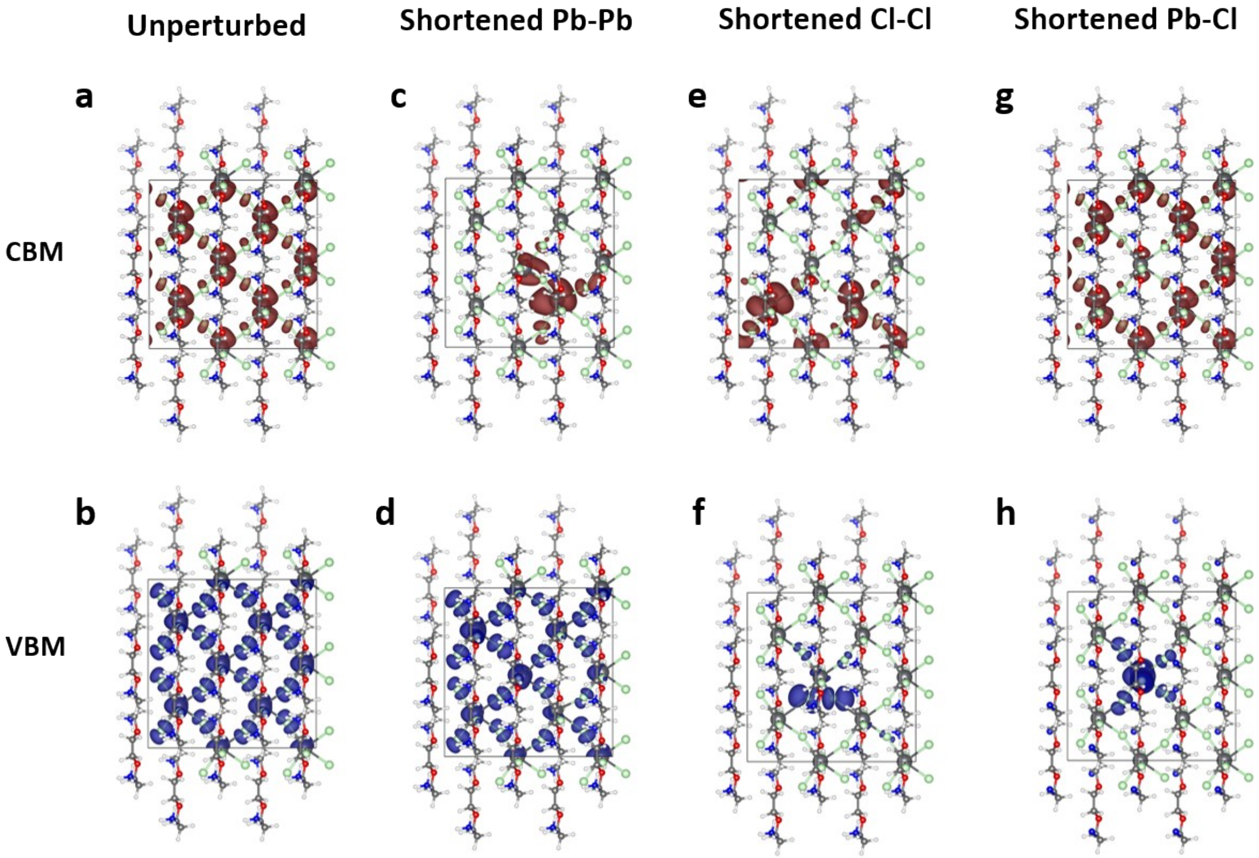

Figure S9| Plots of charge densities of (EDBE)$PbCl_4$ calculated at the PBE/wSOC level. The figures represent the conduction band minimum (CBM) and valence band maximum (VBM) distributions in the unperturbed crystal structure (**a, b**), and upon application of a perturbation. These perturbations involve the shortening of the following atomic distances: Pb-Pb (**c, d**); Cl-Cl (**e, f**); Pb-Cl (**g, h**). Strong charge localization is induced selectively by the applied lattice distortion, compared to the fully delocalized unperturbed system.

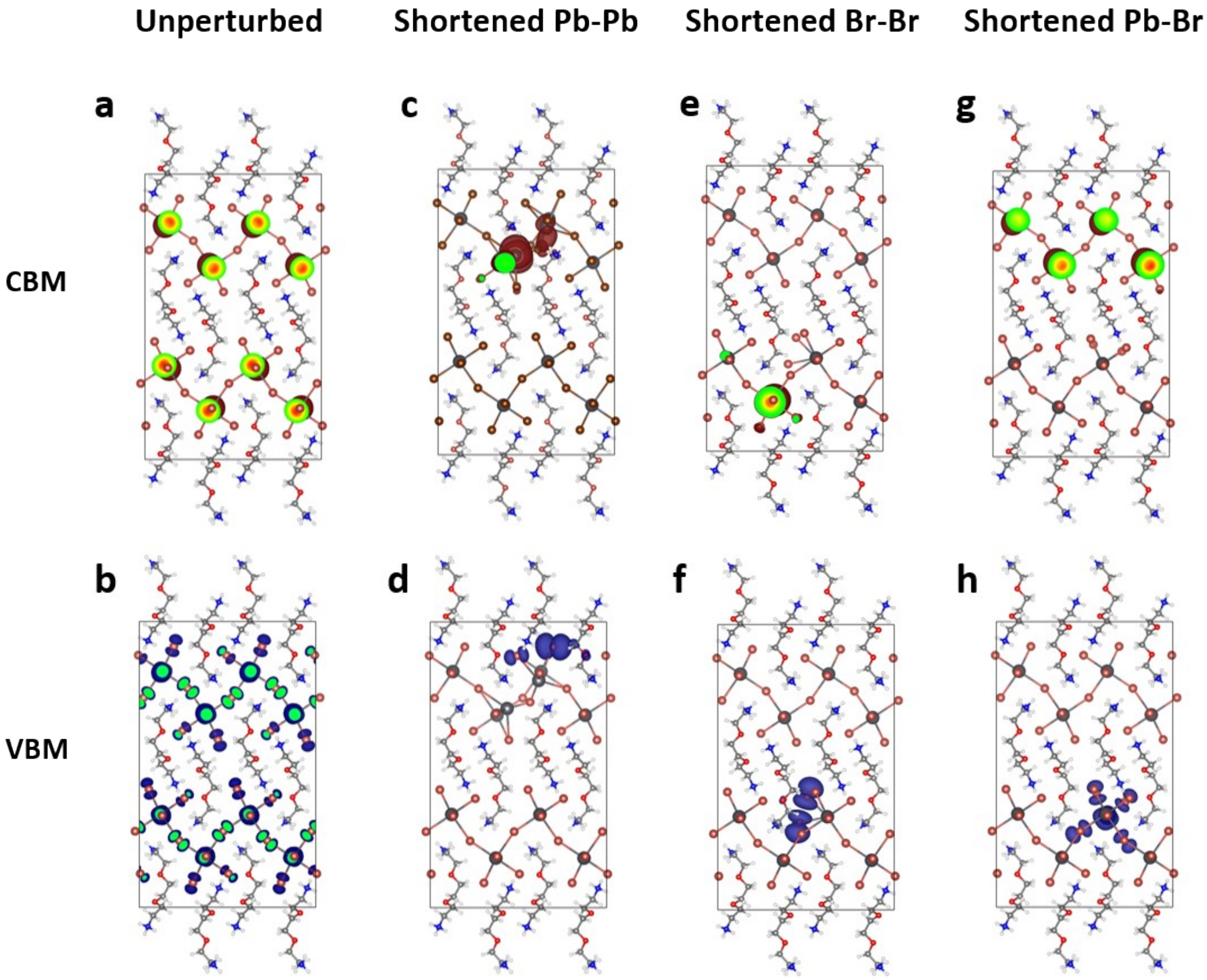

Figure S10| Plots of charge densities of (EDBE)PbBr$_4$ calculated at the PBE/wSOC level. The figures represent the conduction band minimum (CBM) and valence band maximum (VBM) distributions in the unperturbed crystal structure (**a, b**), and upon application of a perturbation. These perturbations involve the shortening of the following atomic distances: Pb-Pb (**c, d**); Br-Br (**e, f**); Pb-Br (**g, h**). Strong charge localization is induced selectively by the applied lattice distortion, compared to the fully delocalized unperturbed system.

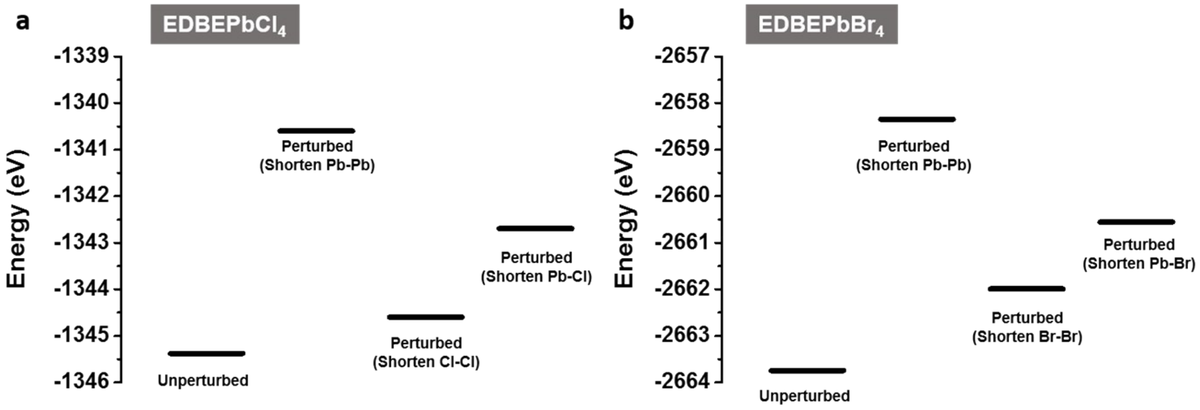

Figure S11| Calculated energies at the PBE/wSOC level for the unperturbed and perturbed crystal structures of **a,** (EDBE)PbCl$_4$ and **b,** (EDBE)PbBr$_4$.

V. References

1. P. J. Brown, D. S. Thomas, A. Köhler, J. S. Wilson, J.-S. Kim, C. M. Ramsdale, H. Sirringhaus and R. H. Friend, *Physical Review B*, 2003, **67**, 064203.
2. M. Pope and C. E. Swenberg, *Electronic Processes in Organic Crystals*, Clarendon Press, 1982.